HHS Public Access

Author manuscript

FEBS Lett. Author manuscript; available in PMC 2021 June 24.

Published in final edited form as:

FEBS Lett. 2020 July ; 594(14): 2322–2330. doi:10.1002/1873-3468.13811.

The Neuronal Transcription Factor Myt1L Interacts via a Conserved Motif with the PAH1 domain of Sin3 to Recruit the Sin3L/Rpd3L Histone Deacetylase Complex

Ryan Dale Marcum, **Ishwar Radhakrishnan**[*]

Department of Molecular Biosciences, Northwestern University, Evanston, Illinois 60208-3500, USA

Abstract

The Sin3L/Rpd3L HDAC complex is one of six major HDAC complexes in the nucleus and its recruitment by promoter-bound transcription factors is an important step in many gene transcription regulatory pathways. Here we investigate how the Myt1L zinc finger transcription factor, important for neuronal differentiation and the maintenance of neuronal identity, recruits this complex at the molecular level. We show that Myt1L, through a highly conserved segment shared with its paralogs, engages directly and specifically with the Sin3 PAH1 domain, targeting the canonical hydrophobic cleft found in PAH domains. Our findings are relevant not only for other members of the Myt family but also for enhancing our understanding of the rules of protein-protein interactions involving Sin3 PAH domains.

Keywords

Histone deacetylases; transcriptional repression; protein-protein interaction; solution NMR spectroscopy; structure-function analysis; repressor-corepressor interaction; neuronal differentiation

Introduction

Chromatin-modifying complexes play critical roles in regulating target gene expression by introducing or erasing post-translational modifications that lead to environments that are permissive or non-permissive to gene transcription [1–3]. The mammalian Sin3L/Rpd3L HDAC complex is one of six constitutively nuclear HDAC complexes that regulates a broad spectrum of targets important for growth, development, differentiation as well as maintenance of cellular identity [4–7]. The complex is recruited directly or indirectly by a wide variety of transcription factors bound sequence-specifically to target promoters. These factors act in large part to effect transcriptional repression through HDAC-mediated removal of the acetyl moiety in acetyllysine-containing chromatin substrates [8, 9].

[*]Corresponding author: Mailing address: 2205 Tech Drive, Department of Molecular Biosciences, Northwestern University, Evanston, Illinois 60208-3500, USA, Tel: +1 847 467-1173; Fax: +1 847 467-6489; i-radhakrishnan@northwestern.edu.

The Sin3 proteins, Sin3A and Sin3B, play critical scaffolding roles in the Sin3L/Rpd3L HDAC complex but are also themselves direct physical targets for recruitment by transcription factors [4]. Prominent examples of transcription factors that do so include the Mxd family of Myc antagonists [10–12], Krüppel-like factors that function as repressors [13, 14], the cell cycle and Wnt pathway regulator, HBP1 [15], the TGF-β signaling pathway regulator, TGIF [16], the neuronal factor, REST/NRSF [17, 18], and the methylcytosine dioxygenases, Tet1 and Tet3 [19], among others. These transcription factors engage with one of two paired amphipathic helix (PAH) domains near the N-terminus of the Sin3 proteins [4].

In this report, we describe the mechanism of Sin3 recruitment by the myelin transcription (Myt) factor family that comprises three members including Myt1, Myt1L (Myt1-like), and Myt3 (also known as ST18) that have been implicated in repressing non-neuronal genes in neural progenitor cells and activating the differentiation program [20, 21]. Both Myt1 and Myt1L have been implicated in repressing transcription via an HDAC-dependent mechanism that involves the recruitment of the Sin3L/Rpd3L complex [21, 22]. Sin3 recruitment by Myt1L was shown to be especially critical for effecting transdifferentiation *in vitro* and for the maintenance of neuronal identity following differentiation [21]. These studies mapped the Myt1L Sin3-interaction domain (SID) to a ~150-residue segment immediately N-terminal to two CCHC-type zinc finger motifs involved in DNA-binding. Here we define the minimal regions of Myt1L and Sin3 necessary and sufficient for direct physical interactions. We further characterize the interaction by solution NMR, fluorescence anisotropy, and mutagenesis, define the molecular basis of and propose a structural model for the interaction.

Materials and Methods

Production of Sin3 and Myt1L proteins

Recombinant mouse Sin3A proteins corresponding to the individual PAH1 and PAH2 domains or spanning both domains were expressed as GST-fusion proteins and purified as described previously [23]. A new mouse Sin3A PAH1 construct (residues 119 to 195) was sub-cloned into the pMCSG7 vector and was expressed and purified as described previously [23]. Human Myt1L constructs spanning amino acid residues 193 to 340 and 193 to 214 were generated as maltose-binding protein (MBP) fusion proteins by sub-cloning the corresponding coding regions into the pMCSG23 vector. Constructs encoding mutant proteins with single amino acid changes were generated using the QuikChangeII site-directed mutagenesis protocol. All constructs were verified by DNA sequencing. Expression of Myt1L MBP-fusion proteins in BL21(DE3) cells was induced using 1 mM IPTG for 16 h at 16 °C. Cell pellets were resuspended in lysis buffer (50 mM Tris, pH 7.9, 400 mM NaCl, 1 mM TCEP, and 1 mM EDTA) supplemented with 0.2% Triton X-100 and a protease inhibitor cocktail comprising 1 mM PMSF, 1 μM leupeptin, and 1 mM pepstatin, bound to amylose resin (New England Biolabs), washed extensively with high-salt buffer (50 mM Tris, pH 7.9, 600 mM NaCl, 1 mM TCEP, and 1 mM EDTA), and eluted with elution buffer (10 mM maltose, 50 mM Tris, pH 7.9, 400 mM NaCl, 1 mM TCEP, and 1 mM EDTA).

For NMR studies, the Myt1L$^{193-214}$ peptide was released from the MBP tag by treating the eluted fractions above with TEV protease overnight at 4 °C while dialyzing against the lysis buffer to remove maltose and passed through the amylose column again to remove MBP. The flow-through was then subjected to reversed-phase HPLC on a C18 column to isolate the desired peptide. The identity and integrity of the peptide were further verified by electrospray ionization-mass spectrometry (ESI-MS).

GST- and MBP-pulldown assays

The individual GST- and MBP-fusion proteins were immobilized on glutathione Sepharose (GE Healthcare) or amylose resins and presented with purified MBP- or GST-fusion proteins, respectively in pulldown buffer (50 mM Tris, pH 7.9, 400 mM NaCl, 1 mM TCEP and 1 mM EDTA). After 1 h incubation at 4 °C, bound proteins were washed five times with pulldown buffer. The resin was then resuspended in SDS-PAGE loading buffer and boiled. Samples were resolved by SDS-PAGE and visualized by staining with Coomassie Brilliant Blue, G-250.

NMR sample generation and spectroscopy

^{15}N and/or ^{15}N,^{13}C-labeled samples of Sin3A PAH1, Sin3B PAH1, Sin3A PAH2 and Sin3B PAH2 were generated using protocols described previously [23]. Freeze-dried Sin3 proteins were dissolved in 20 mM sodium phosphate buffer (pH 6.0) containing 10% D_2O and the pH was adjusted to 6.0 before NMR measurements. Protein concentrations were determined spectrophotometrically [24].

NMR data were acquired on a Bruker Neo 600 spectrometer at 35 °C. For assigning the backbone resonances of free and Myt1L-bound Sin3A PAH1, 2D ^{1}H-^{15}N HSQC, 3D HNCO, HNCACB, and CBCA(CO)NH spectra were acquired. Data processing and analysis were performed using nmrPipe [25] and NMRFAM-Sparky [26]. Sequence-specific backbone resonance assignments were made using PINE [27], but corrections and additional validations were made manually.

Fluorescence anisotropy

A peptide corresponding to amino acid residues 193 to 214 of human Myt1L and bearing a carboxytetramethylrhodamine (TAMRA) moiety conjugated at the N-terminus was chemically synthesized using automated approaches and purified by reversed-phase HPLC. The identity and integrity of the peptide were verified by ESI-MS. Fluorescence data were acquired at room temperature using a Tecan Infinite M1000 microplate reader at 520/590 nm (excitation/emission wavelengths). The assays were performed in triplicate using freshly made samples each time. The anisotropy data were fitted using Kaleidagraph software with the limiting anisotropies and the dissociation constant recovered as free parameters from the fits.

Results and Discussion

Mapping the domain of Sin3A involved in Myt1L interactions

Myt1L was previously shown to recruit the Sin3L HDAC complex by physically interacting with the full-length Sin3B protein [21]. However, the precise Sin3 domain targeted by Myt1L was not defined in these studies. Since the N-terminal PAH1 and PAH2 domains of Sin3 are commonly targeted by multiple transcription factors, we surmised that one or both domains might be directly involved in these interactions. Therefore, we generated a bacterial expression construct corresponding to Myt1L residues 193 to 340 shown by the same study as being both necessary and sufficient for direct interactions with Sin3B and tested this construct for binding to the N-terminal PAH domains. Whereas a GST fusion protein bearing both PAH1 and PAH2 domains of Sin3B as well as the one encompassing only the PAH1 domain bound comparably and efficiently to Myt1L$^{193-340}$, the GST-Sin3B PAH2 construct, like the GST negative control, failed to do so (Figure 1A). To independently verify the specificity of the interaction, ^{15}N-labeled Sin3B PAH1 and Sin3B PAH2 NMR samples were produced and tested for binding to Myt1L$^{193–340}$. Whereas the Sin3B PAH1 NMR spectrum showed widespread perturbations upon Myt1L$^{193-340}$ addition, the NMR spectrum of Sin3B PAH2 remained essentially the same both in the absence and presence of Myt1L$^{193-340}$ (Figure 1B), in line with the pulldown results. Collectively, these results establish the Sin3B PAH1 domain as the sole, direct target of Myt1L interactions.

It is noteworthy that Myt1L, despite sharing little or no sequence similarity, functions like another neural transcription factor REST/NRSF that also recruits the same Sin3L/Rpd3L HDAC complex by directly engaging with the Sin3 PAH1 domain [28]. However, these factors appear to function in a complementary manner in completely different tissues [29]; whereas REST/NRSF is active in non-neuronal tissues, repressing transcription of neuronal genes, Myt1L functions in neuronal progenitors, playing a critical role in neuronal differentiation by selectively repressing transcription of non-neuronal genes [21].

Defining the minimal Sin3-interaction domain of Myt1L

To further define the minimal region of Myt1L involved in efficient interactions with the PAH1 domain, pulldown assays were conducted with purified GST-Sin3A PAH1 and immobilized MBP or MBP fusion proteins Myt1L$^{193-340}$ and Myt1L$^{193–214}$. The latter Myt1L construct was designed because it harbored a highly conserved segment shared by the Myt family (see below). Whereas the MBP negative control failed to bind Sin3A PAH1, both Myt1L constructs bound PAH1 comparably, implying that the shorter Myt1L construct harbored all the key affinity determinants for the interaction (Figure 2A). Additionally, these results confirmed that the Sin3A PAH1 domain, just like Sin3B PAH1 with which it shares 77% sequence identity and 85% sequence similarity, could also engage with Myt1L.

Sequence analyses revealed that the minimal 22-residue SID is highly conserved among Myt family members (Figure 2B). Although the pattern of sequence conservation and its relationship to previously defined Sin3 PAH1-interaction motifs was not readily apparent (but see below), secondary structure prediction methods including PSI-PRED and RaptorX predicted helical conformations with high confidence for the vast majority of residues in this

segment. Since helical conformations are a recurring theme for segments that engage with Sin3 PAH domains [11, 15, 28, 30–33], our sequence analyses collectively suggest that Myt1L SID likely engages with the Sin3 PAH1 domain through a potentially novel interaction motif while adopting a helical conformation.

To obtain quantitative insight into the affinity of the Myt1L-Sin3 interaction, a Myt1L peptide harboring the minimal SID and conjugated with a rhodamine derivative was synthesized for fluorescence anisotropy assays. Titrations with increasing amounts of GST-Sin3A PAH1 while monitoring the changes in fluorescence anisotropy yielded a binding isotherm characteristic of single-site binding (Figure 2C). Non-linear least squares regression yielded an equilibrium dissociation constant (K_d) of 6.0 ± 0.9 μM from three independent measurements, implying a moderate affinity interaction.

Mapping the Myt1L SID binding site within Sin3A PAH1

To gain deeper insights into the mode of Sin3 PAH1 engagement by Myt1L, a 22-residue peptide spanning residues 193 to 214 was expressed and purified. An equimolar complex of the peptide was generated with an $^{15}N,^{13}C$-labeled sample of Sin3A PAH1. Sequence-specific backbone resonance assignments for Sin3A PAH1 in the apo and Myt1L SID-bound states performed using standard triple-resonance approaches followed by PECAN-based analysis of PAH1 chemical shifts revealed four helices at similar locations in previously solved structures ([28, 31, 34]; Supplementary Figure S1). The four-helix core domain is followed by a short segment in an extended conformation, as was previously noted for Sin3B PAH1 [28].

The Myt1L SID peptide produced widespread, yet specific changes in the ^{1}H-^{15}N correlated spectrum of Sin3A PAH1 (Figure 3A). Mapping the chemical shift perturbations onto a previously solved structure of Sin3A PAH1 revealed the prominent hydrophobic cleft on the surface of this domain as the principal binding site for the SID ([31]; Figure 3B). The widespread nature of the perturbations is consistent with and reflective of the cavernous hydrophobic cleft that encompasses all four helices in the structure. PECAN-based secondary structure predictions for residues in Myt1L SID-loaded PAH1, especially near the N-termini of the α1 and α3 helices, the C-termini of the α2 and α4 helices and the extended segment near the C-terminus of the protein, is characterized by increased probabilities for the associated secondary structural element when compared with the predictions for the apo PAH1. These observations are suggestive of and in line with localized folding or stabilization reported previously for Sin3A PAH1 upon SID binding [31]; we note that most of these aforementioned regions constitute the binding site for the SID peptide.

A molecular model for the Myt1L SID-Sin3A PAH1 interaction

Although further insights into the mode of Sin3A PAH1 engagement were precluded by severe exchange broadening effects noted for many Myt1L SID side chain resonances, the helical conformation predicted for the SID along with its targeting of the canonical PAH-binding site, not unlike other SIDs, encouraged us to explore and test potential models of the interaction. Compared to the PAH2 domain, the number of *bona fide* interactors for the PAH1 domain have been far fewer with the neural transcription factor, REST/NRSF, and the

specificity factor, SAP25, constituting the earliest examples [28, 31]. Early structural studies of these two proteins defined two contrasting modes of SID binding to Sin3 PAH1 domains. A key difference between these modes relates to the directionality of the principal interaction motifs that, in turn, is correlated with the helical orientation of the SID relative to the PAH1 domain. The Type I PAH1-interaction motif ϕ-x-ϕ-ϕ-s-x-ϕ-s (where ϕ=bulky hydrophobic; x=any non-proline residue; s=any residue with a short side chain) described for REST/NRSF is distinct from the Type II motif s-ϕ-x-s-ϕ-ϕ-x-ϕ described for SAP25 [31], which more recently was shown to be shared by the Tet1/Tet3 transcription factors that function in embryonic stem cells [19].

Assuming the pattern of sequence conservation noted for the SIDs of the Myt family is reflective of the PAH1-interaction motif (Figure 2B), no obvious relationship could be discerned between this pattern and the Type I motif and neither does the conservation pattern strictly follow the Type II motif. However, relaxing the constraints especially for the positions occupied by bulky hydrophobic residues in the Type II motif yielded two candidates, one for the Myt1L segment ^{201}VAKSLLNL^{208} and another involving an overlapping segment ^{204}SLLNLGKI^{211}. To distinguish between these modes, which will be referred to as Mode 1 and Mode 2, respectively, we mutated residues predicted by the corresponding models to play key roles in dictating the affinity of the Myt1L-Sin3A interaction. In Mode 1, V201 is predicted to occupy a position normally occupied by residues with short side chains while A202 is predicted to occupy a position normally occupied by bulky hydrophobic residues. Therefore, we asked whether V201A and/or A202L would serve to enhance the affinity of the interaction over the wild-type protein. Pulldown assays showed binding by both mutants to GST-Sin3A PAH1 but only at a level comparable to the wild-type protein (Figure 4A).

Since L205 and L208 play key roles in both Mode 1 and Mode 2, we mutated L205 to glutamic acid and tested this mutant for binding activity. In line with expectation, the L205E mutant failed to bind efficiently to GST-Sin3A PAH1 in the pulldown assay (Figure 4A). To definitively distinguish between the two modes, we then asked whether I211 had a role in stabilizing the Myt1L-Sin3A complex. Whereas this residue has no role in Mode 1, it plays a critical role in Mode 2. In the pulldown assay, an I211E mutant, like L205E, failed to bind GST-Sin3A PAH1 efficiently (Figure 4A), implicating I211 as a key affinity determinant and lending decisive support for Mode 2.

We modeled the Myt1L-Sin3A complex based on the previously reported NMR structure of the SAP25-Sin3A complex ([31]; Figure 4B). Even though the Myt1L and SAP25 SIDs share little sequence similarity, the structure-function analyses above allowed alternative modes of engagement to be interrogated and equivalent residues in the two SIDs to be established (Figure 4C). Although most of the changes to the SAP25 SID sequence could be readily accommodated without adverse steric clashes in the model by selecting a commonly occurring side chain rotamer conformation for each residue, incorporation of Myt1L N207 in place of a glycine residue required translation of the SID helix by ~0.5 Å towards helix α1 of PAH1. Indeed, G209 located on the opposite face of the SID helix in place of a bulky hydrophobic residue called for by the Type II motif readily allows for this possibility. Furthermore, both V201A and A202L mutations could be readily accommodated in the

context of this model, with the side chain of the former residue targeting a hydrophobic patch while that of the latter is exposed to the solvent (Figure 4B), explaining why these mutants did not produce any deleterious effects on PAH1 binding.

An important principle to emerge from the studies described above is that whereas bulky, hydrophobic residues at certain locations of the Type II interaction motif are vital, deviations from the canonical motif – as most vividly illustrated by Myt1L N207 and G209 – are tolerated so long as there are compensatory changes elsewhere. Indeed, these deviations from the canonical motif might partly explain why the affinity of Sin3A PAH1 for Myt1L SID is about 40-fold lower than the corresponding value measured for SAP25 SID [31].

A key feature of protein-protein interactions involving Sin3 PAH domains is the high level of specificity exhibited by the interactors. Although the PAH3 domain is distantly related to the N-terminal PAH domains at the sequence and structural levels [32], the PAH1 and PAH2 domains share a high degree of sequence similarity even at the level of residues that are typically involved in making intermolecular contacts (Supplementary Figure S2). Although our studies of Myt1L reinforce the notion of the highly specific nature of interactions involving PAH domains (Figure 1), the basis for its preference for PAH1 over PAH2 remains to be explored. We do note that in previous studies, seemingly subtle changes (*e.g.*, V→L, L→M, N→D, Y→F) at the protein-protein interface played a profound role in dictating PAH1 versus PAH2 specificity [31]; we anticipate the same residues playing a similar role in promoting or diminishing Myt1L interactions.

Conclusions

In conclusion, we have described a novel, highly-conserved protein-protein interaction motif shared by members of the Myt family of neural transcription factors that facilitates the recruitment of the constitutively nuclear Sin3L/Rpd3L HDAC complex to repress target genes. Myt proteins lacking the motif were previously shown by genetic studies to be defective in effecting neuronal differentiation and our studies provide a mechanistic understanding of how the motif functions at the molecular level. Specifically, we showed that the motif directly engages the PAH1 domain of the scaffolding proteins Sin3A and Sin3B in the HDAC complex in a manner reminiscent of previously characterized interactors including SAP25 and Tet1/Tet3. A key principle to emerge from our studies is that small but significant deviations from previously characterized interaction motifs accompanied by compensatory changes could continue to support the interaction. Since PAH-interaction motifs are typically very short, spanning less than a dozen residues, this plasticity which ensures engagement with multiple, unrelated factors also has the effect of considerably raising the informatics challenges of precisely and accurately identifying the segment involved in protein-protein interactions. We anticipate that an approach that balances *in silico* analyses with targeted experiments like the one described herein will be indispensable for addressing these types of challenges.

Supplementary Material

Refer to Web version on PubMed Central for supplementary material.

Acknowledgements:

This work was supported by grants from the American Heart Association to I.R. (17GRNT33680167) and R.D.M. (16PRE27260041) and from an H-Foundation grant to I.R. awarded by the Robert H. Lurie Comprehensive Cancer Center at Northwestern University. We are grateful to Marius Wernig (Stanford) for providing Myt1L cDNA and to Yongbo Zhang for assistance with NMR data collection.

Abbreviations:

HDAC	histone deacetylase
SID	Sin3 interaction domain
PAH	paired amphipathic helix domain
CSP	chemical shift perturbation

References

1. Bannister AJ & Kouzarides T (2011) Regulation of chromatin by histone modifications, Cell Res. 21, 381–395. [PubMed: 21321607]
2. Gardner KE, Allis CD & Strahl BD (2011) OPERating ON Chromatin, a Colorful Language where Context Matters, J Mol Biol. 409, 36–46. [PubMed: 21272588]
3. Jenuwein T & Allis CD (2001) Translating the histone code, Science. 293, 1074–1080. [PubMed: 11498575]
4. Adams GE, Chandru A & Cowley SM (2018) Co-repressor, co-activator and general transcription factor: the many faces of the Sin3 histone deacetylase (HDAC) complex, Biochem J. 475, 3921–3932. [PubMed: 30552170]
5. Hayakawa T & Nakayama J (2011) Physiological roles of class I HDAC complex and histone demethylase, Journal of biomedicine & biotechnology. 2011, 129383. [PubMed: 21049000]
6. Watson PJ, Fairall L & Schwabe JW (2012) Nuclear hormone receptor co-repressors: structure and function, Mol Cell Endocrinol. 348, 440–449. [PubMed: 21925568]
7. Grzenda A, Lomberk G, Zhang JS & Urrutia R (2009) Sin3: master scaffold and transcriptional corepressor, Biochim Biophys Acta. 1789, 443–450. [PubMed: 19505602]
8. Seto E & Yoshida M (2014) Erasers of histone acetylation: the histone deacetylase enzymes, Cold Spring Harb Perspect Biol. 6, a018713. [PubMed: 24691964]
9. Yang XJ & Seto E (2008) The Rpd3/Hda1 family of lysine deacetylases: from bacteria and yeast to mice and men, Nat Rev Mol Cell Biol. 9, 206–218. [PubMed: 18292778]
10. Laherty CD, Yang WM, Sun JM, Davie JR, Seto E & Eisenman RN (1997) Histone deacetylases associated with the mSin3 corepressor mediate Mad transcriptional repression, Cell. 89, 349–356. [PubMed: 9150134]
11. Brubaker K, Cowley SM, Huang K, Loo L, Yochum GS, Ayer DE, Eisenman RN & Radhakrishnan I (2000) Solution structure of the interacting domains of the Mad-Sin3 complex: implications for recruitment of a chromatin-modifying complex, Cell. 103, 655–665. [PubMed: 11106735]
12. Eilers AL, Billin AN, Liu J & Ayer DE (1999) A 13-amino acid amphipathic alpha-helix is required for the functional interaction between the transcriptional repressor Mad1 and mSin3A, J Biol Chem. 274, 32750–32756. [PubMed: 10551834]
13. Zhang JS, Moncrieffe MC, Kaczynski J, Ellenrieder V, Prendergast FG & Urrutia R (2001) A conserved alpha-helical motif mediates the interaction of Sp1-like transcriptional repressors with the corepressor mSin3A, Mol Cell Biol. 21, 5041–5049. [PubMed: 11438660]
14. Pang YP, Kumar GA, Zhang JS & Urrutia R (2003) Differential binding of Sin3 interacting repressor domains to the PAH2 domain of Sin3A, FEBS Lett. 548, 108–112. [PubMed: 12885416]

15. Swanson KA, Knoepfler PS, Huang K, Kang RS, Cowley SM, Laherty CD, Eisenman RN & Radhakrishnan I (2004) HBP1 and Mad1 repressors bind the Sin3 corepressor PAH2 domain with opposite helical orientations, Nat Struct Mol Biol. 11, 738–746. [PubMed: 15235594]
16. Wotton D, Knoepfler PS, Laherty CD, Eisenman RN & Massague J (2001) The Smad transcriptional corepressor TGIF recruits mSin3, Cell Growth Diff. 12, 457–463. [PubMed: 11571228]
17. Huang Y, Myers SJ & Dingledine R (1999) Transcriptional repression by REST: recruitment of Sin3A and histone deacetylase to neuronal genes, Nat Neurosci. 2, 867–872. [PubMed: 10491605]
18. Naruse Y, Aoki T, Kojima T & Mori N (1999) Neural restrictive silencer factor recruits mSin3 and histone deacetylase complex to repress neuron-specific target genes, Proc Natl Acad Sci U S A. 96, 13691–13696. [PubMed: 10570134]
19. Chandru A, Bate N, Vuister GW & Cowley SM (2018) Sin3A recruits Tet1 to the PAH1 domain via a highly conserved Sin3-Interaction Domain, Sci Rep. 8, 14689. [PubMed: 30279502]
20. Vasconcelos FF, Sessa A, Laranjeira C, Raposo A, Teixeira V, Hagey DW, Tomaz DM, Muhr J, Broccoli V & Castro DS (2016) MyT1 Counteracts the Neural Progenitor Program to Promote Vertebrate Neurogenesis, Cell Rep. 17, 469–483. [PubMed: 27705795]
21. Mall M, Kareta MS, Chanda S, Ahlenius H, Perotti N, Zhou B, Grieder SD, Ge X, Drake S, Euong Ang C, Walker BM, Vierbuchen T, Fuentes DR, Brennecke P, Nitta KR, Jolma A, Steinmetz LM, Taipale J, Sudhof TC & Wernig M (2017) Myt1l safeguards neuronal identity by actively repressing many non-neuronal fates, Nature. 544, 245–249. [PubMed: 28379941]
22. Romm E, Nielsen JA, Kim JG & Hudson LD (2005) Myt1 family recruits histone deacetylase to regulate neural transcription, J Neurochem. 93, 1444–1453. [PubMed: 15935060]
23. He Y & Radhakrishnan I (2008) Solution NMR studies of apo-mSin3A and mSin3B reveal that the PAH1 and PAH2 domains are structurally independent, Protein Sci. 17, 171–175. [PubMed: 18042683]
24. Gill SC & von Hippel PH (1989) Calculation of protein extinction coefficients from amino acid sequence data, Anal Biochem. 182, 319–326. [PubMed: 2610349]
25. Delaglio F, Grzesiek S, Vuister GW, Zhu G, Pfeifer J & Bax A (1995) NMRPipe: a multidimensional spectral processing system based on UNIX pipes, J Biomol NMR. 6, 277–293. [PubMed: 8520220]
26. Lee W, Tonelli M & Markley JL (2015) NMRFAM-SPARKY: enhanced software for biomolecular NMR spectroscopy, Bioinformatics. 31, 1325–1327. [PubMed: 25505092]
27. Lee W, Westler WM, Bahrami A, Eghbalnia HR & Markley JL (2009) PINE-SPARKY: graphical interface for evaluating automated probabilistic peak assignments in protein NMR spectroscopy, Bioinformatics. 25, 2085–2087. [PubMed: 19497931]
28. Nomura M, Uda-Tochio H, Murai K, Mori N & Nishimura Y (2005) The neural repressor NRSF/REST binds the PAH1 domain of the Sin3 corepressor by using its distinct short hydrophobic helix, J Mol Biol. 354, 903–915. [PubMed: 16288918]
29. Hwang JY & Zukin RS (2018) REST, a master transcriptional regulator in neurodegenerative disease, Curr Opin Neurobiol. 48, 193–200. [PubMed: 29351877]
30. Spronk CA, Tessari M, Kaan AM, Jansen JF, Vermeulen M, Stunnenberg HG & Vuister GW (2000) The Mad1-Sin3B interaction involves a novel helical fold, Nat Struct Biol. 7, 1100–1104. [PubMed: 11101889]
31. Sahu SC, Swanson KA, Kang RS, Huang K, Brubaker K, Ratcliff K & Radhakrishnan I (2008) Conserved themes in target recognition by the PAH1 and PAH2 domains of the Sin3 transcriptional corepressor, J Mol Biol. 375, 1444–1456. [PubMed: 18089292]
32. Xie T, He Y, Korkeamaki H, Zhang Y, Imhoff R, Lohi O & Radhakrishnan I (2011) Structure of the 30-kDa Sin3-associated protein (SAP30) in complex with the mammalian Sin3A corepressor and its role in nucleic acid binding, J Biol Chem. 286, 27814–27824. [PubMed: 21676866]
33. Kumar GS, Xie T, Zhang Y & Radhakrishnan I (2011) Solution structure of the mSin3A PAH2-Pf1 SID1 complex: a Mad1/Mxd1-like interaction disrupted by MRG15 in the Rpd3S/Sin3S complex, J Mol Biol. 408, 987–1000. [PubMed: 21440557]

34. Eghbalnia HR, Wang L, Bahrami A, Assadi A & Markley JL (2005) Protein energetic conformational analysis from NMR chemical shifts (PECAN) and its use in determining secondary structural elements, J Biomol NMR. 32, 71–81. [PubMed: 16041485]

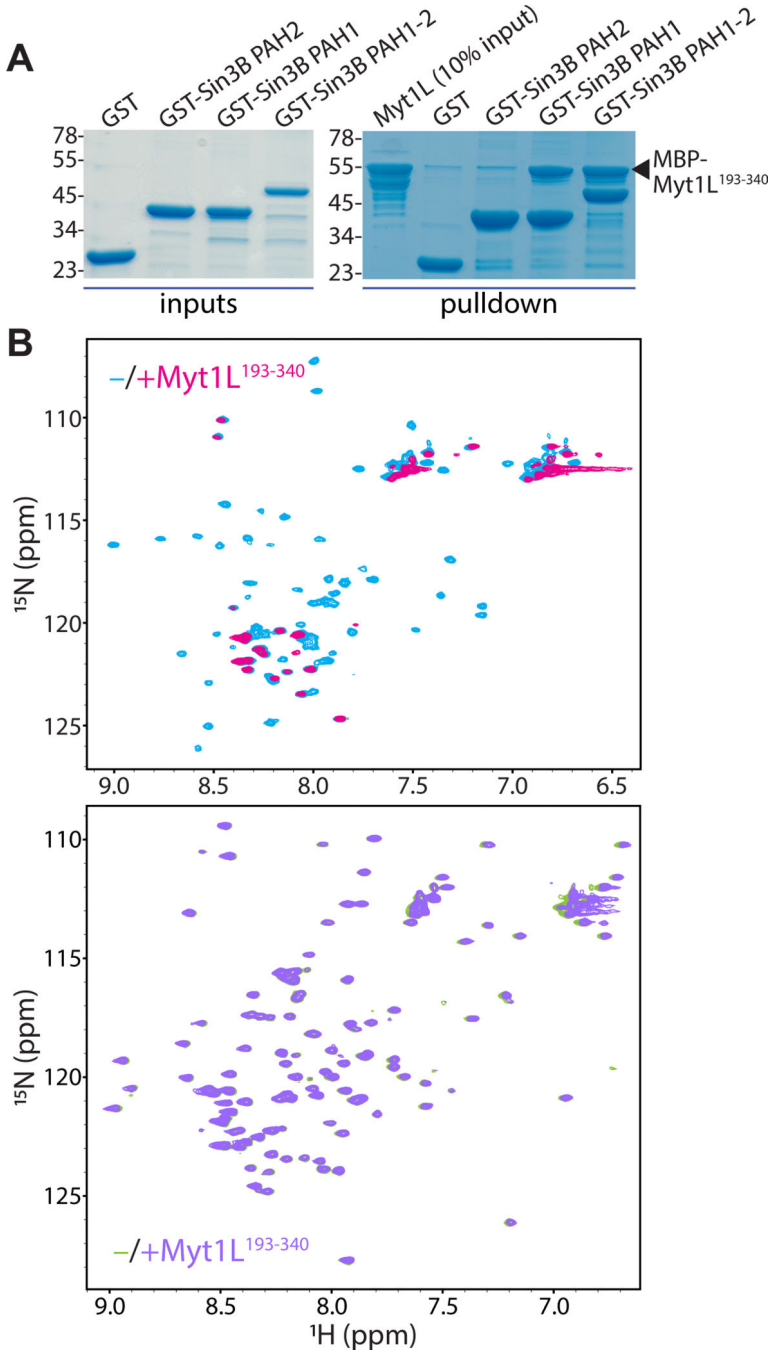

Figure 1.

Myt1L engages the Sin3B PAH1 domain in direct physical interactions. (**A**) SDS-PAGE analyses of immobilized GST and GST-fusion proteins encompassing the PAH1 and/or PAH2 domains of Sin3B that were used as inputs for the GST-pulldown assays (*left panel*) and following the pulldown assays with MBP-tagged Myt1L$^{193–340}$ (*right panel*). The bands in these gels were visualized by staining with Coomassie Brilliant Blue G-250. (**B**) ^{1}H-^{15}N correlated spectra of ^{15}N-labeled Sin3B PAH1 recorded in the absence (cyan) and presence (magenta) of one equivalent of unlabeled Myt1L$^{193–340}$ (*top panel*) and those of ^{15}N-labeled

Sin3B PAH2 recorded in the absence (green) and the presence (purple) of one equivalent of unlabeled Myt1L$^{193-340}$ (*bottom panel*). The NMR spectra were recorded at 35 °C at a protein concentration of 0.2–0.4 mM in 20 mM sodium phosphate buffer, pH 6.0.

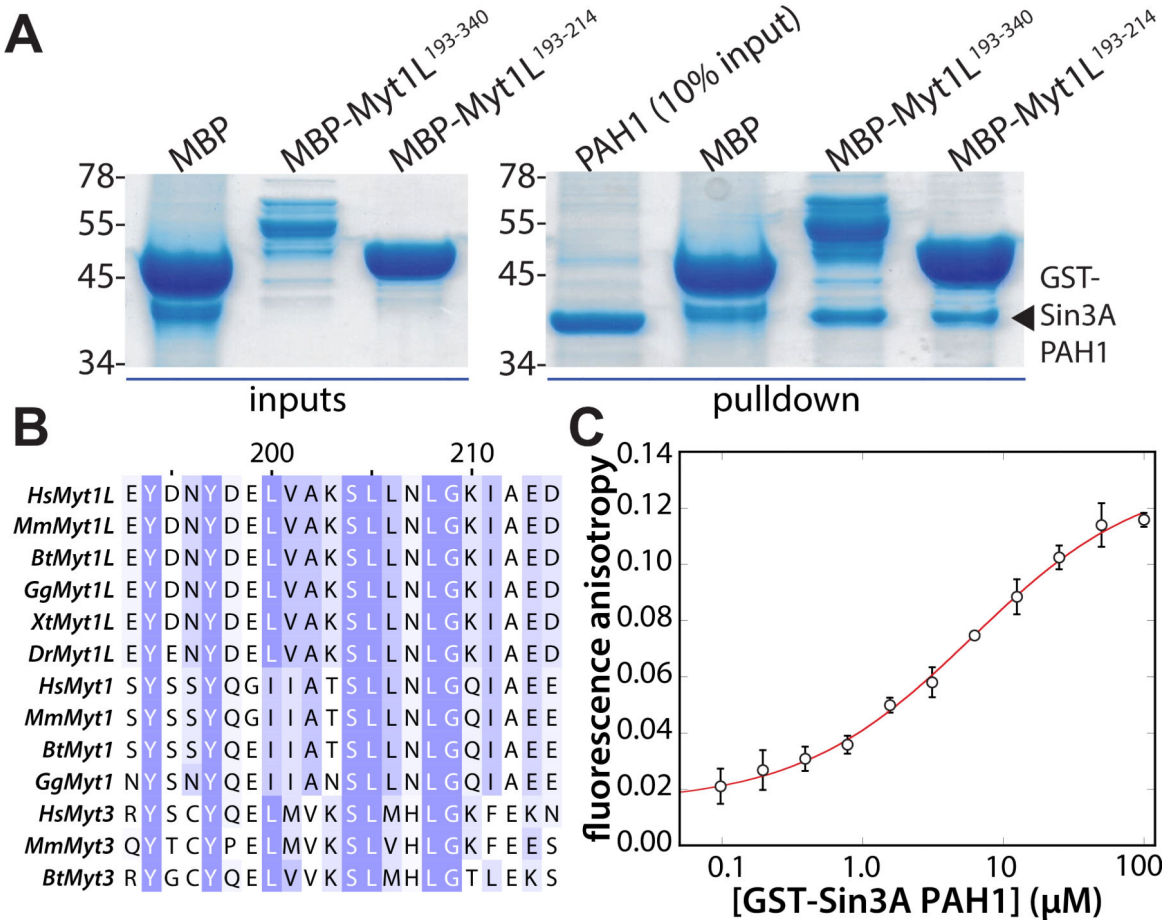

Figure 2.

A highly conserved segment shared by the Myt family constitutes the minimal Sin3-interaction domain (SID). (**A**) SDS-PAGE analyses of the immobilized MBP and MBP-fusions of Myt1L that were used as inputs for the MBP-pulldown assays (*left panel*) and following the pulldown assays with GST-tagged Sin3A PAH1 (*right panel*). (**B**) A CLUSTAL Ω guided multiple sequence alignment of the SIDs of Myt family members from various species. Species abbreviations: Hs: *Homo sapiens*; Mm: *Mus musculus*; Bt: *Bos taurus*; Gg: *Gallus gallus*; Xt: *Xenopus tropicalis*; Dr: *Danio rerio*. Conserved residues are shaded according to the level of conservation and how well dissimilar residues score in the BLOSUM62 matrix. (**C**) A representative binding isotherm from fluorescence anisotropy assays conducted by titrating 5 nM of TAMRA-conjugated Myt1L$^{193-214}$ SID peptide with varying concentrations of purified GST-tagged Sin3A PAH1. Non-linear least-squares fitting yielded the following parameters: initial anisotropy, A_0 = 0.015±0.002; final anisotropy, A_∞ = 0.132±0.005; equilibrium dissociation constant, K_d = 6.0 ± 0.9 μM.

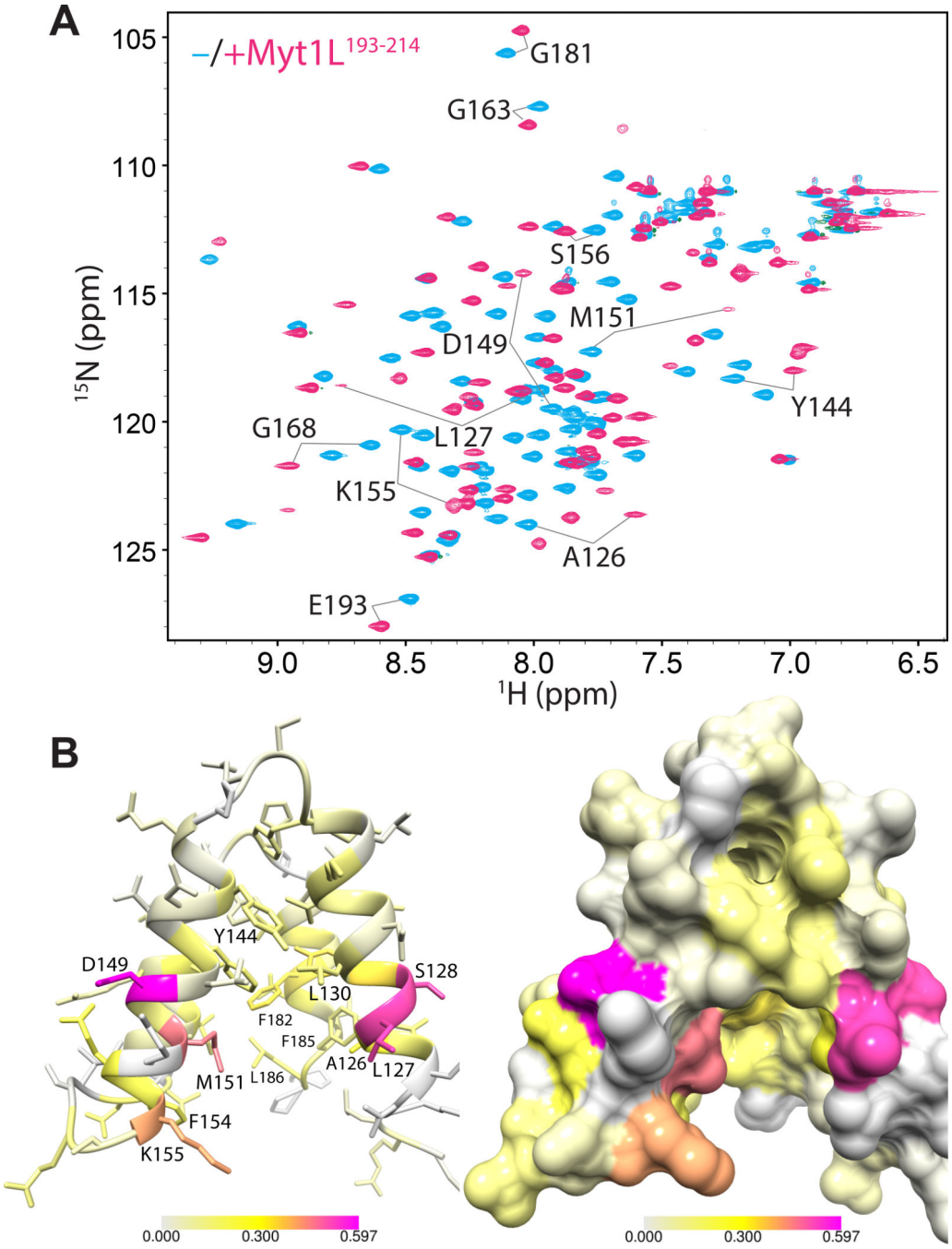

Figure 3.

Myt1L SID targets the canonical binding site in Sin3A PAH1. (**A**) ^{1}H-^{15}N correlated spectra of ^{15}N,^{13}C-labeled Sin3A PAH1 in the absence (light blue) and presence (magenta) of one equivalent of Myt1L$^{193–214}$ SID peptide. The NMR spectra were recorded at 35 °C at a protein concentration of 0.4 mM in 20 mM sodium phosphate buffer, pH 6.0. (**B**) Two views of the NMR chemical shift perturbations (CSPs) mapped on to the backbone (*left panel*) and the molecular surface of the Sin3A PAH1 domain (*right panel*; PDB accession: 2RMS; [31]). The perturbations were calculated using the equation: CSP = $\sqrt{(0.5*((\delta_{HN,bound} -$

$\delta_{HN,free})^2 + 0.04*(\delta_{N,bound} - \delta_{N,free})^2)$). The colors yellow and magenta in the heat map respectively denote CSPs (in ppm) that are one and three standard deviations above the average value; colors are linearly interpolated for the intermediate values. Because of solvent- or ligand-induced resonance broadening, the backbone resonances for the following residues could not be assigned in one or both states: K122, V123, E124, K152, I159, and M180; therefore, their CSPs were set to zero.

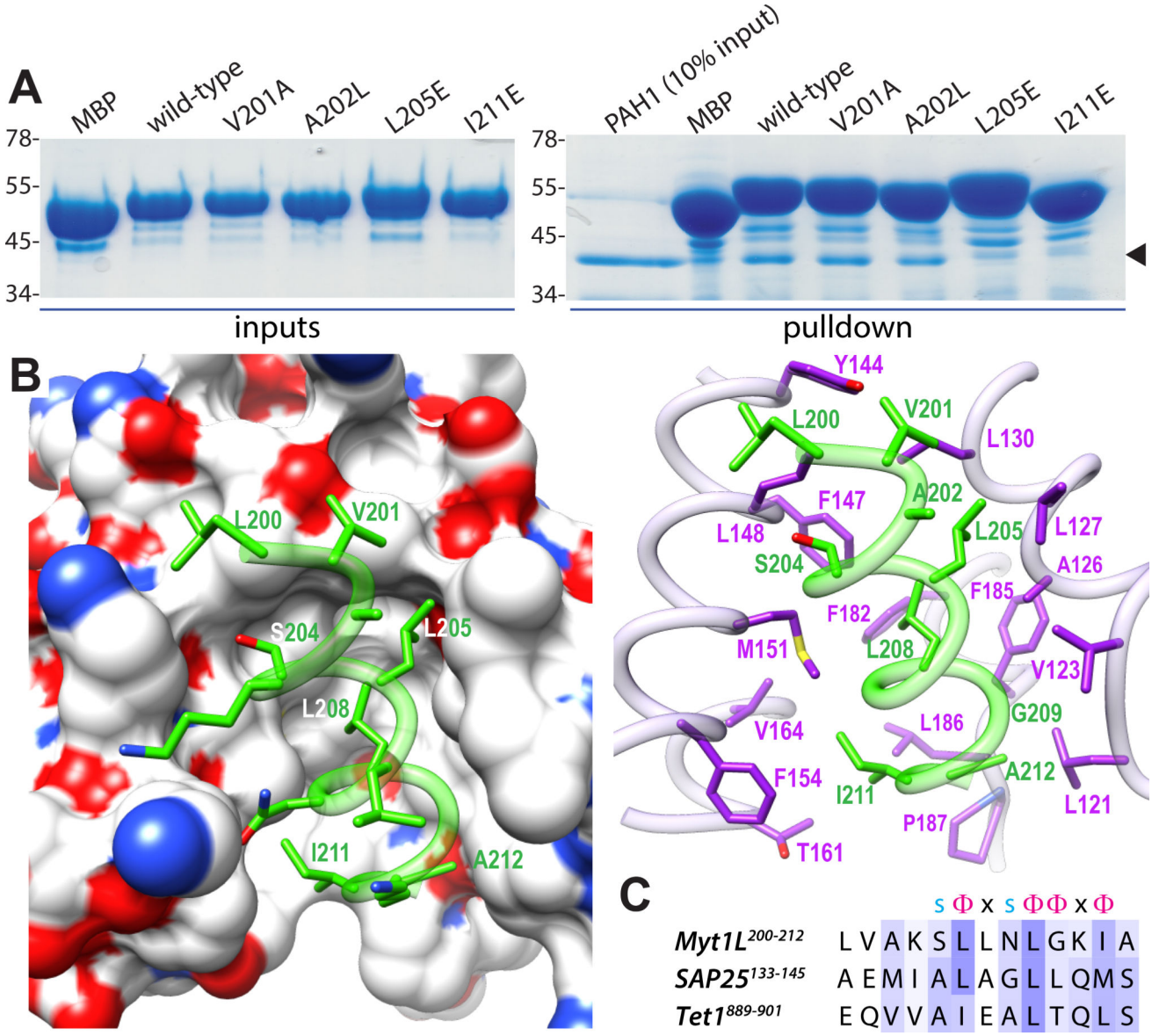

Figure 4.

A molecular model for the interaction between Sin3A PAH1 and Myt1L SID. (**A**) MBP-pulldown assays probing the role of various Myt1L residues at the protein-protein interface. SDS-PAGE analyses of immobilized, purified MBP and MBP-fusions of Myt1L that were used as inputs for the MBP-pulldown assays (*left panel*) and following the pulldown assays with GST-tagged Sin3A PAH1 (*right panel*). The arrowhead on the right marks the expected location of GST-Sin3A PAH1. (**B**) A model for the Myt1L-Sin3A interaction based on the previously solved solution structure of the SAP25-Sin3A complex. Residues in the helical segment of Myt1L SID (in green) presumed to engage with a deep hydrophobic cleft in the Sin3A PAH1 domain (rendered as a molecular surface; *left panel*). For clarity, only the polypeptide backbone of the interacting segments along with side chains of interfacial residues are shown in the molecular model (*right panel*). (**C**) A multiple sequence alignment

comparing the sequences of diverse transcription factors that engage similarly with the PAH1 domain.